1 **Lack of cyclophilin D protects against the development of acute lung injury in**

2 **endotoxemia**

3 Fruzsina Fonai[1], Janos K. Priber[1], Peter B. Jakus[1], Nikoletta Kalman[1], Csenge Antus[1], Edit

4 Pollak[2], Gergely Karsai[2], Laszlo Tretter[3], Balazs Sumegi[1,4,5], Balazs Veres[1,*]

5 [1] Department of Biochemistry and Medical Chemistry, Medical Faculty, University of Pecs,

6 Pecs, Hungary

7 [2] Department of Comparative Anatomy and Developmental Biology, Faculty of Sciences,

8 University of Pecs, Pecs, Hungary

9 [3] Department of Medical Biochemistry, Semmelweis University, Budapest, Hungary

10 [4] Szentagothai Research Center, University of Pecs, Pecs, Hungary

11 [5] MTA-PTE Nuclear and Mitochondrial Interactions Research Group, Pecs, Hungary

12 [*]**Corresponding author**: Balazs Veres, Department of Biochemistry and Medical Chemistry,

13 University of Pecs Medical School, 12 Szigeti str., H-7624 Pecs, Hungary; Tel.: 36(72)536-

14 276; Fax.: 36(72)536-277; E-mail: balazs.veres@aok.pte.hu

15

Abstract

Sepsis caused by LPS is characterized by an intense systemic inflammatory response affecting the lungs, causing acute lung injury (ALI). Dysfunction of mitochondria and the role of reactive oxygen (ROS) and nitrogen species produced by mitochondria have already been proposed in the pathogenesis of sepsis; however, the exact molecular mechanism is poorly understood. Oxidative stress induces cyclophilin D (CypD)-dependent mitochondrial permeability transition (mPT), leading to organ failure in sepsis. In previous studies mPT was inhibited by cyclosporine A which, beside CypD, inhibits cyclophilin A, B, C and calcineurin, regulating cell death and inflammatory pathways. The immunomodulatory side effects of cyclosporine A make it unfavorable in inflammatory model systems. To avoid these uncertainties in the molecular mechanism, we studied endotoxemia-induced ALI in CypD$^{-/-}$ mice providing unambiguous data for the pathological role of CypD-dependent mPT in ALI. Our key finding is that the loss of this essential protein improves survival rate and it can intensely ameliorate endotoxin-induced lung injury through attenuated proinflammatory cytokine release, down-regulation of redox sensitive cellular pathways such as MAPKs, Akt, and NF-κB and reducing the production of ROS. Functional inhibition of NF-κB was confirmed by decreased expression of NF-κB-mediated proinflammatory genes. We demonstrated that impaired mPT due to the lack of CypD reduces the severity of endotoxemia-induced lung injury suggesting that CypD specific inhibitors might have a great therapeutic potential in sepsis-induced organ failure. Our data highlight a previously unknown regulatory function of mitochondria during inflammatory response.

1. Introduction

Sepsis is a severe systemic inflammatory process caused by bacterial agents, such as lipopolysaccharide (LPS). LPS plays a crucial role in the induction of inflammatory responses and acute lung injury (ALI), leading to acute respiratory distress syndrome (ARDS) [1, 2]. The binding of LPS to toll-like receptor (TLR) 4 initiates signaling pathways, culminating in the activation of mitogen-activated protein kinases (MAPK) and NF-κB [3, 4]. As a consequence of NF-κB activation, the expression of cytokines and chemokines is up-regulated, causing neutrophil infiltration into the lung [5, 6, 7]. Leukocytes produce reactive oxygen species (ROS) and nitrogen monoxide (NO), in order to eliminate pathogens. However, the excessive production of these reactive agents can damage cellular components and lead to epithelial and endothelial cell death and tissue damage. LPS-induced ROS can further enhance the activity of redox-sensitive inflammatory transcription factors and signaling kinases such as MAPKs and Akt [8-11].

Cytosolic Ca^{2+} overload or ROS can trigger the opening of mitochondrial permeability transition (mPT) pore leading to the collapse of ATP production, release of proapoptotic molecules and initiating further ROS production. Cyclophilin D (CypD), a matrix peptidyl-prolyl cis-trans-isomerase, encoded by the nuclear Ppif gene, is a modulator of mPT although the exact molecular composition of the pore is still under debate [12, 13]. Studies with mitochondria lacking CypD demonstrated very low Ca^{2+}-sensitivity and delayed mPT pore opening, clearly favoring an indispensable modulatory role of CypD [14, 15, 13]. The generally used inhibitor of mPT is cyclosporine A (CsA) [16] which inhibits, not only CypD, but also cyclophilin A, B, C and calcineurin, therefore has a wide range of signaling effects – including inflammatory signaling - unrelated to CypD [17-20]. Thus, immunomodulatory effects of CsA make it unfavorable for investigating the role of mPT under inflammatory conditions. The role of mPT has been implicated in many pathological conditions accompanied by oxidative damage; however, there are only a few studies regarding the role of mPT in inflammatory processes, and no experiment has been conducted to date to evaluate its participation in ALI. Here, we give the first specific evidence for the role of CypD-dependent mPT in ALI using CypD knock-out mice.

2. Materials and methods

2.1. Ethics Statement

Animal experiments were performed according to Hungarian Governmental Regulation 40/2013. (II. 14.) in accordance to the Directive 2010/63/EU of the European Parliament and of the Council on the protection of animals used for scientific purposes. The license was approved by the County Governmental Office (No. BA02/2000-20/2011) lasting for five years (2013-2017).

2.2. Animals

Male C57BL/6 mice were from Charles River Hungary Breeding and genetically engineered homozygous male Ppif-/- cyclophilin D knock-out mice with C57BL/6 background were supplied by Prof. László Tretter (Semmelweis University, Budapest, Hungary). The mice were kept under standard conditions.

2.3. Materials

LPS from Escherichia coli 0127:B8 and all materials that are not specified elsewhere were purchased from Sigma-Aldrich (St. Louis, MO). Anti-phospho-p44/42, anti-p44/42, anti-phospho-Akt, anti-Akt, anti-phospho-p38, anti-p38, anti-phospho-JNK, anti-JNK, anti-phospho-NF-κB p65, anti-NF-κB p65, anti-phospho-IκBα and anti-IκBα primary antibodies for immunoblotting were from Cell Signaling Technology (Danvers, MA), anti-MKP-1, anti-4-hydroxy-2-noneal Michael adducts, anti-nitrotyrosine and anti-GAPDH antibodies were from Millipore (Billerica, MA).

2.4. ALI model and survival study

To induce murine endotoxemia, intraperitoneal LPS (40 mg/kg, dissolved in PBS) was given, control groups received PBS (10 μl/g). Primarily survival study was performed with age–matched wild type (n=8) and CypD knock-out mice. Mice were monitored for clinical signs of endotoxemia and lethality every hour for 96 h, after that they were monitored 3 times a day

till the end of the first week. No late deaths were observed in any of the experimental groups. Alternatively, 24 hours after treatment the mice were anesthetized with isoflurane (Isopharma). Lungs were removed, and processed as follows: the right upper lobe was fixed in 10% paraformaldehyde, except for a piece which was put into primary fixative (2% paraformaldehyde / 2% glutaraldehyde) for electronmicroscopy; the right lower lobes were snap frozen in liquid N_2; the left upper lobe was put into RNAlater RNA stabilization reagent (Qiagen, Hilden, Germany); the left lower lobe lung homogenate was prepared as described later.

2.5. Western blot analysis

10 mg of frozen tissue was homogenized (50 mM TRIS, 50 mM EDTA, 50 mM sodium metavanadate, 0.5% protease inhibitor cocktail, 0.5% phosphatase inhibitor cocktail, pH=7.4) and the protein concentration was determined with a DC™ Protein Assay kit (Bio-Rad, Hercules, CA). Western blotting was performed as described previously [9]. Peroxidase labeling was visualized with the Pierce ECL Western Blotting Substrate (Thermo Scientific, Waltham, MA) detection system. Quantification of band intensities of the blots was performed by ImageJ software.

2.6. Cytokine determination by ELISA from lung homogenate

After removal of the left lower lobe, the tissue was rinsed in ice-cold PBS and homogenized. Protein concentration was determined with DC™ Protein Assay kit (Bio-Rad). TNFα, IL-1β and IL-10 concentrations were measured with ELISA Ready-SET-Go! (eBioscience, San Diego, CA): 200 μg protein/well was used, the cytokine-amount was expressed in optical density at 450 nm.

2.7. mRNA isolation from lung tissue and quantitative RT-PCR

RNA was isolated from tissue samples kept in RNALater (Qiagen) solution using TRIzol reagent (Invitrogen, Grand Island, NY). Total RNA concentration was determined using

128   spectrophotometric method (IMPLEN NanoPhotometerTM, München, Germany) and reverse-

129   transcribed into cDNA with MMLV RT / RevertAid™ First Strand cDNA Synthesis Kit

130   (Fermentas, Burlington, Canada). RT-PCR was performed with 1μl of cDNA in MiniOpticon

131   Real-Time PCR System (Bio-Rad) using SYBR Green Supermix kit (Bio-Rad). Specific

132   primers against CD14, IL-1α, Cxcl2, IFN-γ, iNOS, TNFα and actin were used. The relative

133   gene expression was calculated with ΔΔCt method using BIO-RAD CFX Manager software.

134

2.8. Pulmonary histopathology

136   The paraformaldehyde fixed superior lobe of the right lung was embedded in paraffin and cut

137   into 5 μm sections. Hematoxylin-eosin staining was performed using standard protocol. Slides

138   were scored in a double blinded manner by an independent expert using the scoring system

139   described previously [21]. Five slides in each group were assessed under high power field and

140   evaluated for intra-alveolar and interstitial neutrophil accumulation, presence of proteinaceous

141   debris and hyaline membrane, and also alveolar wall thickening.

142

2.9. Immunohistochemistry

144   The lung tissue sections were probed with antibodies against 4-hydroxy-2-noneal Michael

145   adducts and nitrotyrosine. Formalin-fixed, paraffin-embedded 5μm tissue sections were

146   deparaffinized and rehydrated followed by heat-induced epitope retrieval using 97°C heat

147   exposure for 20 min. Sections were incubated in primary antibody over-night. Blocking and

148   staining procedures were performed with Dako EnVision™ FLEX detection system with

149   Dako Autostainer Plus instruments (Glostrup, Denmark). All sections were counterstained

150   with hematoxylin.

151

2.10. Electron microscopy

153   Tissue samples were rinsed in 0.1 M phosphate buffer then fixed in 2 % glutaraldehyde / 2 %

154   paraformaldehyde for 3 hours. After a post-fixation step (osmium tetraoxide 1 % in 0.1 M

155   phosphate buffer) samples were dehydrated and embedded into Durcupan epoxy resin. Serial

156 ultrathin sections were cut and collected on cupper grids, then passed onto drops of uranyl

157 acetate, later on lead citrate. Following the routine counterstaining samples were rinsed in

158 distilled water and dried. Samples were observed and documented with JEOL 1200 (Tokyo,

159 Japan) transmission electron microscope.

160 **2.11. Statistical analysis**

161 Comparisons between experimental groups were made by one-way ANOVA and post-hoc

162 test. Data represent mean ± SEM. A value of $p < 0.05$ was considered statistically significant.

163

164 **3. Results**

165 **3.1. Mice lacking CypD survive lethal endotoxemia**

166 CypD knock-out animals exhibited improved survival rate after intraperitoneal high dose LPS

167 treatment compared to wild type mice. Out of the 8 CypD$^{-/-}$ mice two (25%) died within the

168 first 30 hours but after that no deaths occurred. However all of the 8 wild type mice died

169 within 60 hours (Figure 1). These results show that the loss of CypD massively reduces

170 mortality.



.

171
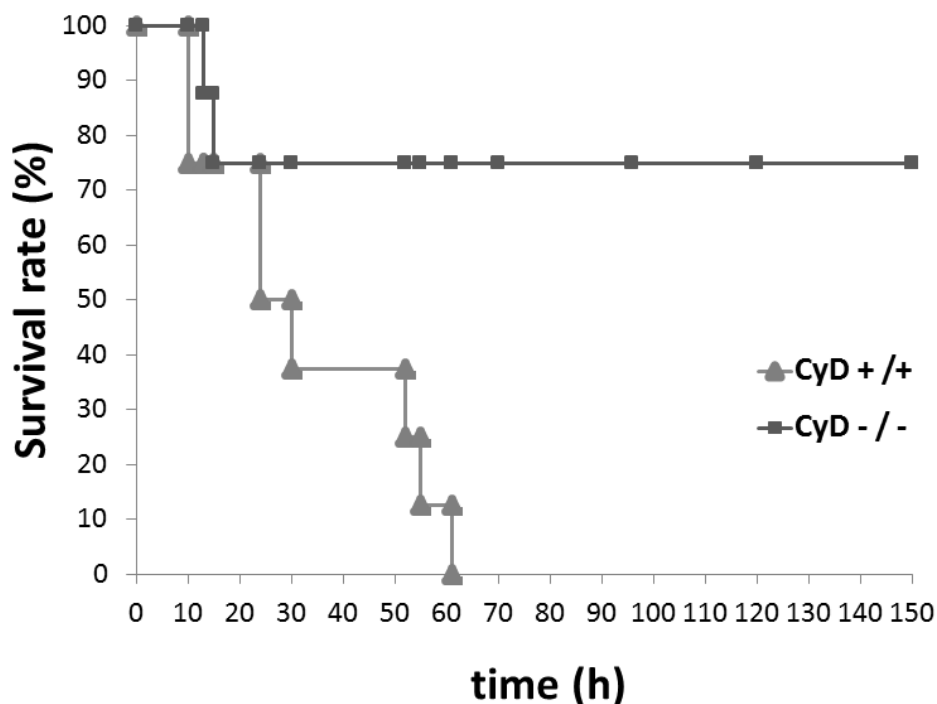
Figure 1. Mice lacking CypD survive lethal endotoxemia. Survival study was carried out with age-matched wild-type (n=8) and CypD knock-out mice (n = 8). Survival was monitored for 7 days, after 40 mg/kg intraperitoneal LPS administration.

3.2. CypD knock-out mice are protected against LPS-induced histopathological changes

Histological examination revealed severe lung injury in LPS-treated wild type animals. On hematoxylin-eosin stained sections, alveolar wall thickening, blood vessel congestion and perivascular exudation were seen, which are suggestive of impaired tissue architecture and function, while robust interstitial neutrophil infiltration indicated ongoing immune response (Figure 2C). Interstitial accumulation of neutrophils was markedly decreased in LPS-treated $CypD^{-/-}$ mice (Figure 2E, 2F). Other pathological changes like alveolar widening and perivascular edema were also significantly milder in $CypD^{-/-}$ lungs and no thrombotic event could be observed despite moderate congestion (Figure 2D). Lungs of control animals in both groups had normal tissue architecture with thin alveolar walls, occasional intra-alveolar macrophages and few neutrophils (Figure 2A, 2B). For making histological examination quantitative a scoring was performed as described earlier (Figure 2G). Scores were significantly higher in the LPS-treated wild type mice compared to CypD knock-outs mainly resulting from marked differences in interstitial neutrophil accumulation and alveolar thickening.

191

192

193
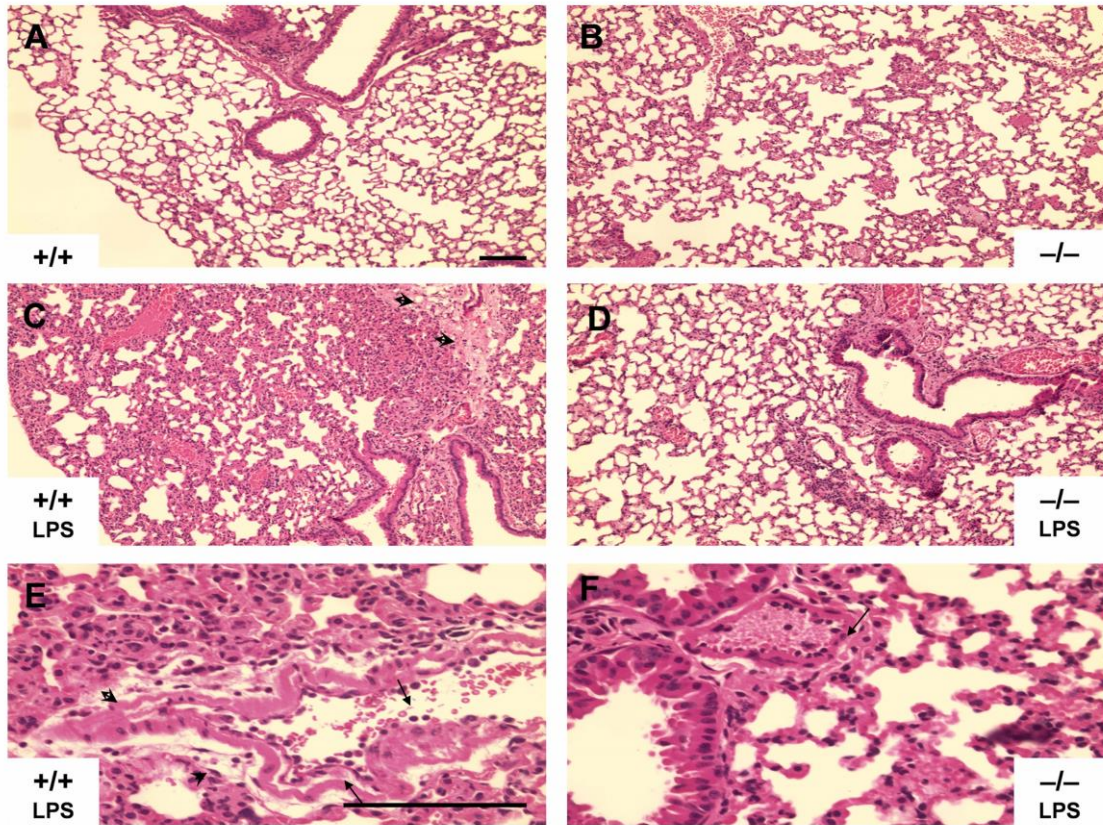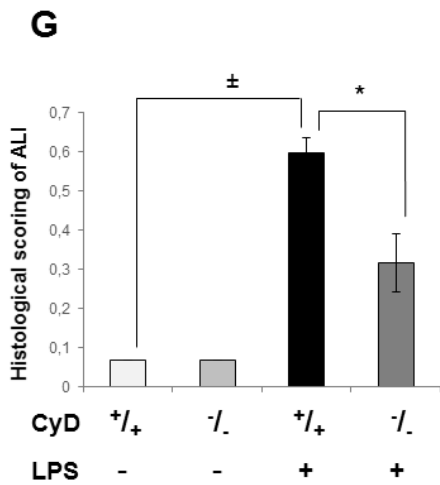
**Figure 2. Deletion of CypD prevents lung vascular permeability, edema, and inflammation induced by LPS.** Representative pathological and histological analysis of lungs from untreated (A) and LPS-treated (C) wild type mice, as well as from untreated (B) and LPS-treated (D) CypD knock-out mice. Enlarged light microscopic images highlight differences of vascular events in LPS-treated wild type (E) and knock-out mice (F). Arrows pointing on marginating and transmigrating leukocytes, arrowheads indicate severe endothelial leakage with consequent perivascular edema. Original magnification was 10X

(A,B,C,D) and 40X (E,F). Scale bars represent 100 μm. Histological scoring was also performed in double blinded manner according to the recommendations of the American Thoracic Society (G). Results are presented as mean ± SEM, n = 5. Significant difference between control and LPS-treated wild type animals is indicated by ± (p < 0.001), significant difference between LPS-treated wild type and CypD knock-out animals is indicated by * (P < 0.05).

3.3. Lack of CypD prevents the fine structural anatomy of lung tissue damaged by LPS

LPS treatment induced serious lesions in the lung tissue of wild type mice. Endothelial cells were swollen loaded with cytoplasmic vacuoles and the number of pinocytotic vesicles was increased (Figure 3C, 3I). Inter-endothelial connections of endothelial cells were damaged or dilated (Figure 3M). An impaired, leaky endothelial layer of blood vessels allowed extravasation of intravascular fluid resulting in tissue edema. Another sign of impaired blood vessel functioning was a detached basal membrane with an unsettled fibroelastic layer in the alveolar septa (Figure 3D). These denuded surfaces are potential targets of fibrin attachment and hyaline membrane formation. The proinflammatory activity of fibrin fragments and massive liberation of immune cell molecules may explain the appearance of a considerable amount of cell debris. Obvious thickening of the alveolar septa by accumulated connective tissue indicates strong fibrosis (Figure 3D). Tissue organization of CypD$^{-/-}$ mice with or without LPS treatment was almost identical to that of wild type untreated animals (Figure 3A, 3B, 3G-L). The level of septal thickening was not comparable to that in wild type LPS-treated animals (Figure 3D, 3E). This observation indicates the quicker resolution of acute lung tissue lesions or much milder tissue injury.
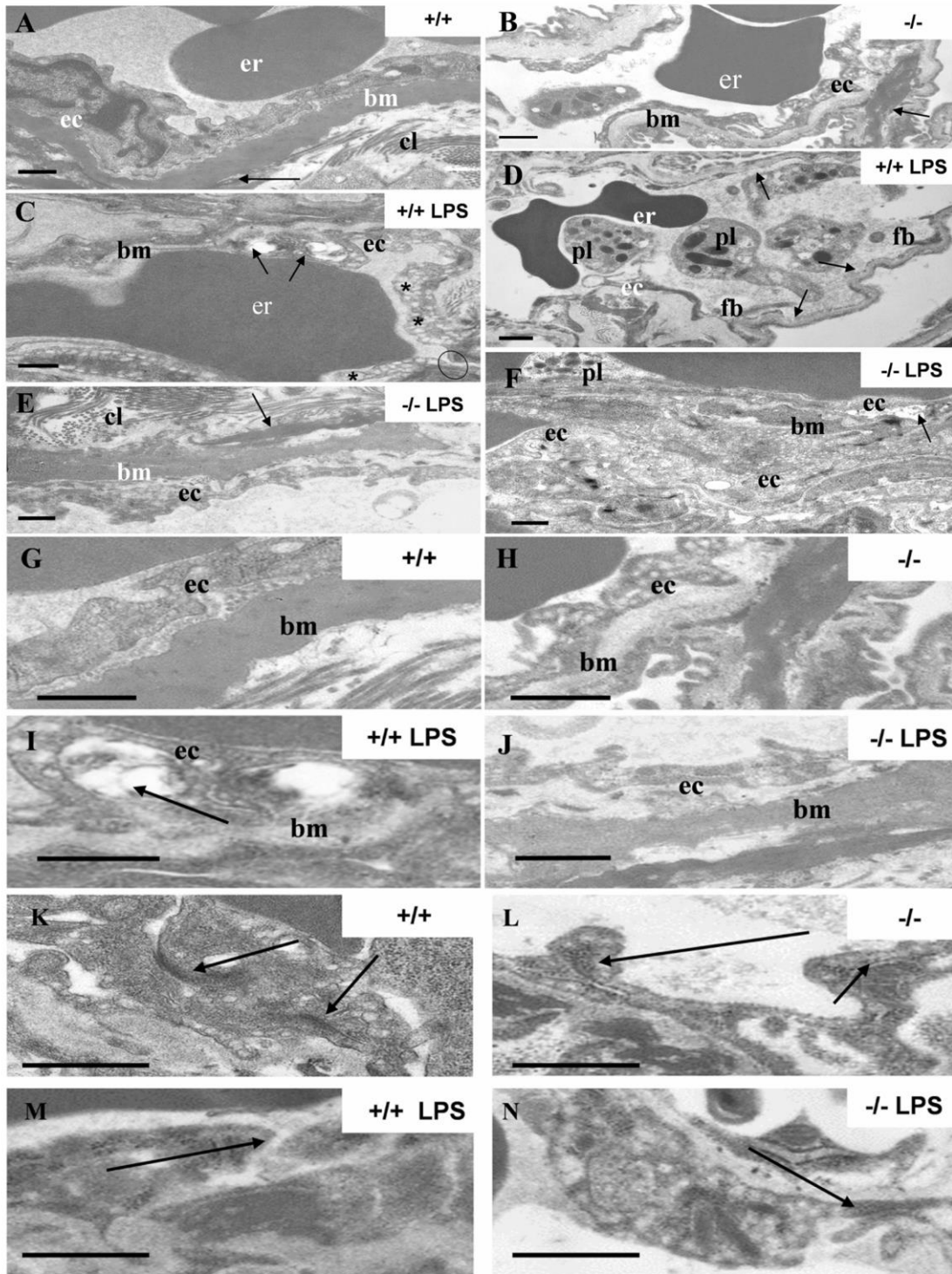
Figure 3. Lack of CypD prevents the fine structural anatomy of lung tissue damaged by LPS. (A) In untreated wild type mice blood vessel endothelial cells (ec) attach intact basement membrane (bm). Dense layer of fibro elastic membrane supports interseptal wall (arrow). er: erythrocyte, cl: collagen fibers. (B) In CypD knock-out mice intact basement membrane (bm) and endothelial cell (ec) are visible. Prominent fibro elastic layer (arrow) lying beneath basement membrane. (C, D) LPS-treated wild type mice show seriously

231 degenerating portion of an endothelial cell (ec) with large vacuoles appearing in cytoplasm

232 (arrows, C) and thinner basement membrane (bm). Number and size of pinocytotic vesicles

233 (stars) are increased, cytoplasm is swollen. Widened inter endothelial junction (circle) is also

234 shown. Portions of endothelial cells are focally detached from basal membrane (arrows, D).

235 Denuded patches serve potential surfaces to fine fibrin branches (fb) to attach. Blood vessel

236 lumen is congested with platelets (pl). (E, F) In CypD knock-out LPS-treated mice the

237 structure of blood vessel walls is almost identical with that of control animals. Intact

238 endothelial cell (ec) basement membrane (bm) and fibro elastic membrane (arrow, E) are

239 shown. Diffuse appearance of collagen fibers (cl) could also be observed. In some cases intact

240 endothelial cell (ec) portions were seen focally detached (arrow, F) from basement membrane

241 (bm). Cytoplasmic swelling could not be seen. (G, H) Fine structure of endothelial cells show

242 no morphological changes between $CypD^{+-+}$ vs $CypD^{-/-}$. (I, J) Serious endothelial cytoplasmic

243 degeneration is visible (arrow, I) in LPS-treated wild type compared to knock-out mice. (K,

244 L) Dense membrane sections of inter endothelial junctions (arrows) in blood vessel walls are

245 intact both in wild type and CypD knock-out control animals. (M, N) Arrows show widened

246 and intact thigh junctions in blood vessel wall of LPS-treated wild type and CypD knock-out

247 animals, respectively. Scale bars: 500 nm.

248

3.4. Loss of CypD protects lung epithelial cells against oxidative damage

250 Lung tissue sections were examined with immunohistochemistry using antibodies against

251 nitrotyrosine, and 4-hydroxy-2-noneal Michael adducts. LPS treatment markedly enhanced

252 immunohistochemical staining in endothelial and lung epithelial cells of wild type animals.

253 Endothelial and epithelial cells of $CypD^{-/-}$ mice showed less intense staining (Figure 4A). The

254 extensive lipid-peroxidation damage after LPS treatment in wild type animals was also visible

255 regarding bronchial mucinosus cells. In contrast, endotoxemic $CypD^{-/-}$ mice exhibited a

256 markedly reduced staining of endothelial tissue, while the intensity of epithelial positivity was

257 almost the same as in wild type and knock-out animals without LPS treatment (Figure 4B).

12

258
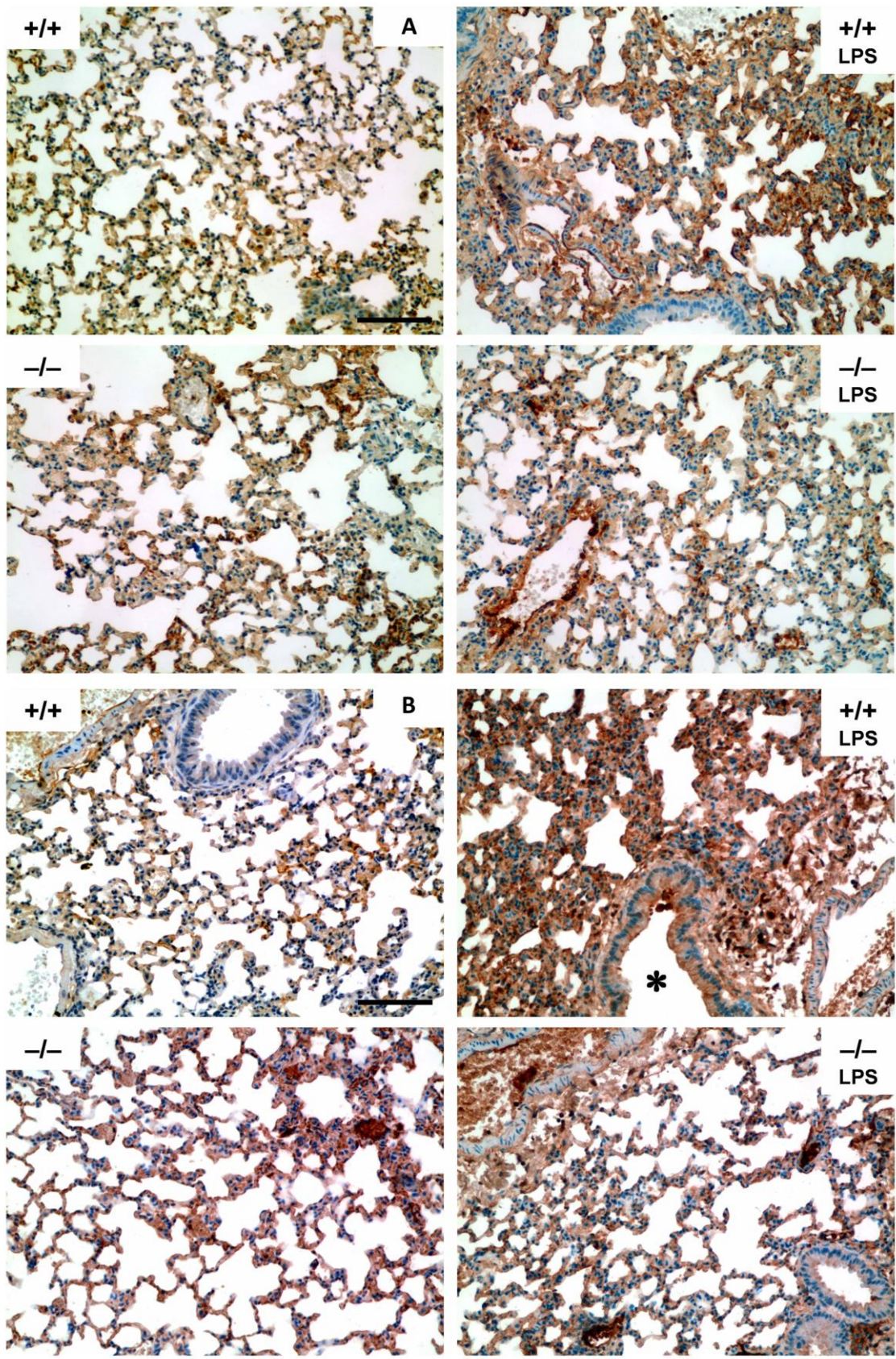
**Figure 4. Loss of CypD protects the lung epithelial cells against oxidative damage.**
Immunohistochemical staining of mouse lungs for nitrotyrosine (A) and for 4-hydroxy-2-

noneal Michael adducts (B) in lung tissue counterstained with hematoxylin. Endothelia of lung vessels in LPS-treated wild type mice were intensively stained compared to CypD knock-out mice. Epithelial cells showed prominent positivity in wild type, but not in knock-out LPS-treated animals. Star indicates airway lumen with strong positivity of bronchial cells and secretory product. Scale bar represents 100 μm.

3.5. Absence of CypD impairs proinflammatory, but does not affect anti-inflammatory cytokine production

During ALI, early phase cytokines promote the production of chemokines by resident cells to enhance neutrophil sequestration into the lung. Clinical studies have proven the importance of these factors, since the outcome of patients with ARDS significantly correlates with the concentration of these cytokines in bronchoalveolar lavage fluid [7, 21, 22]. In our experiments, LPS treatment resulted in elevated TNFα and IL-1β levels, measured in lung homogenates, while the amount of these cytokines was markedly decreased in LPS-treated CypD$^{-/-}$ mice (Figure 5A, 5B). IL-10, responsible for limiting inflammatory processes, ameliorates endotoxemia-induced ALI and high levels in the lungs of patients suffering from ARDS correlated with better outcome [23, 24]. In our study, there was no difference in the amount of anti-inflammatory IL-10 in total lung homogenates between wild type and knock-out animals 24h after LPS administration (Figure 5C), as both increased significantly.
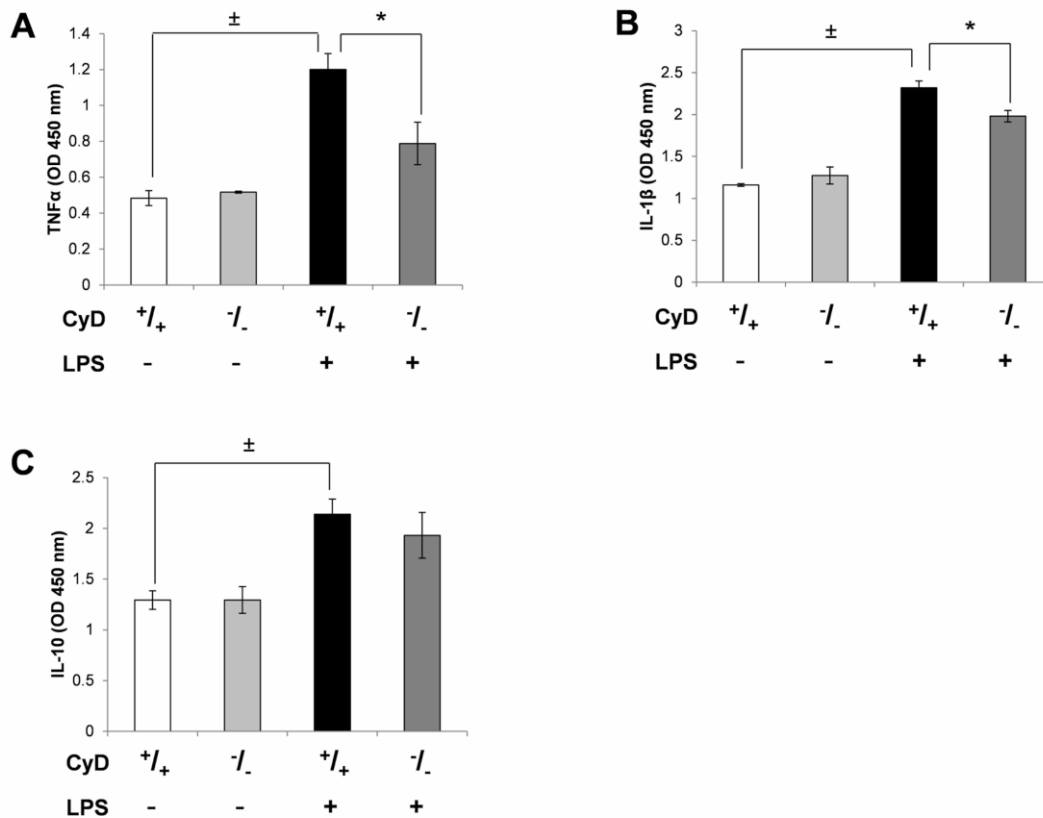
Figure 5. Effect of LPS on cytokine production of wild type and CypD^{-/-} mice. Determination of proinflammatory cytokines TNFα (A) and IL-1β (B), and anti-inflammatory cytokine IL-10 (C) 24 h after LPS-treatment from total lung homogenates by ELISA. Bars represent mean ± SEM of optical densities, n = 4. Significant difference between control and LPS-treated wild type animals is indicated by ± ($p < 0.05$), significant difference between LPS-treated wild type and CypD knock-out animals is indicated by * ($P < 0.05$).

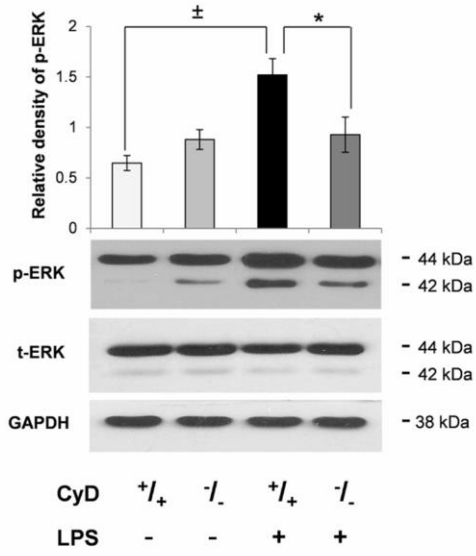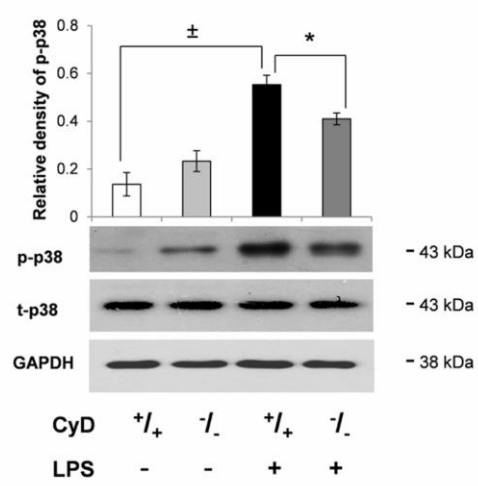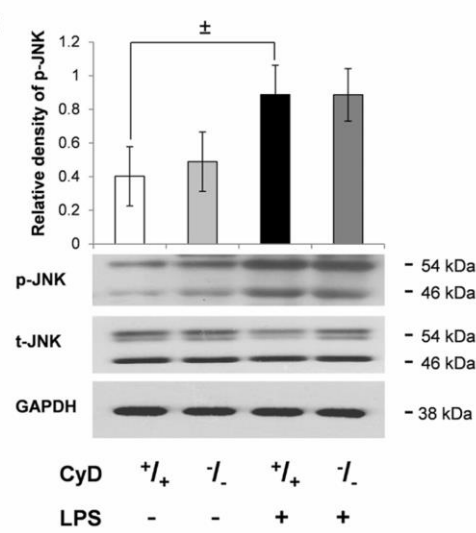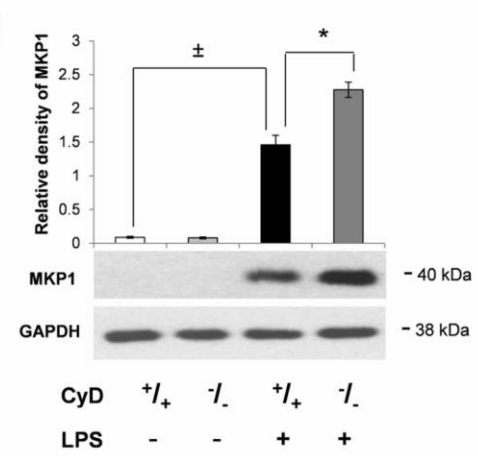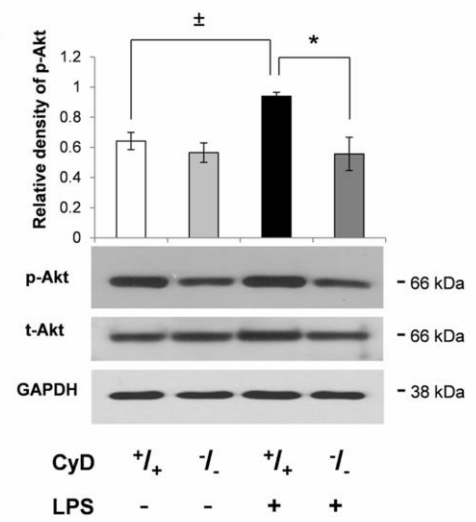**3.6. Deficiency of CypD affects the activation of MAPKs through MKP-1 and Akt in mouse lungs after LPS treatment**

Phosphorylation and activation of MAPKs was shown to play an important role in the development of ALI following LPS exposure [25, 26]. In our experiments, phosphorylation levels of extracellular signal-regulated kinase (ERK), p38, and c-Jun N-terminal kinase (JNK) were significantly elevated 24 hours after LPS treatment in wild type animals, while the activation of ERK and p38 was lower in the lungs of LPS-treated CypD^{-/-} mice (Figure 6A, B). No difference could be observed in JNK phosphorylation between knock-out and wild type animals after LPS challenge (Figure 6C).

297   MAP kinases are under the direct negative regulation through dephosphatase activity of

298   MAPK-phosphatase-1 (MKP1). The level of MKP1 was up-regulated in CypD$^{-/-}$ mice

299   compared to wild type animals after LPS treatment (Figure 6D).

300   Beside MAP kinases Akt contributes to the TLR4 signaling cascade leading to NF-κB

301   activation and promoting inflammatory processes in the lung. In our experiment, LPS

302   treatment significantly enhanced the phosphorylation of Akt in the lungs of wild type animals,

303   while this effect was strongly reduced in CypD$^{-/-}$ animals, resulting in a phosphorylation level

304   that was comparable to that seen in control animals (Figure 6E).

A

Relative density of p-ERK

| CyD | ⁺/₊ | ⁻/₋ | ⁺/₊ | ⁻/₋ |
| LPS | − | − | + | + |

p-ERK — 44 kDa, 42 kDa
t-ERK — 44 kDa, 42 kDa
GAPDH — 38 kDa

B

Relative density of p-p38

| CyD | ⁺/₊ | ⁻/₋ | ⁺/₊ | ⁻/₋ |
| LPS | − | − | + | + |

p-p38 — 43 kDa
t-p38 — 43 kDa
GAPDH — 38 kDa

C

Relative density of p-JNK

| CyD | ⁺/₊ | ⁻/₋ | ⁺/₊ | ⁻/₋ |
| LPS | − | − | + | + |

p-JNK — 54 kDa, 46 kDa
t-JNK — 54 kDa, 46 kDa
GAPDH — 38 kDa

D

Relative density of MKP1

| CyD | ⁺/₊ | ⁻/₋ | ⁺/₊ | ⁻/₋ |
| LPS | − | − | + | + |

MKP1 — 40 kDa
GAPDH — 38 kDa

E

Relative density of p-Akt

| CyD | ⁺/₊ | ⁻/₋ | ⁺/₊ | ⁻/₋ |
| LPS | − | − | + | + |

p-Akt — 66 kDa
t-Akt — 66 kDa
GAPDH — 38 kDa

305

17

Figure 6. Deficiency of CypD affects MAPKs, MKP-1 and Akt in mouse lungs after LPS treatment. Activation of ERK (A), p38 (B), SAPK/JNK (C), MKP-1 (D) and Akt (E) in lung total homogenates was determined 24 h after LPS treatment by immunoblotting utilizing phosphorylation specific and total primary antibodies. Total proteins (non-phosphorylated) and GAPDH were used as loading controls. A representative blot as well as a bar diagram of the quantified blots are presented. Bars represent mean ± SEM of pixel densities, n = 4. Significant difference between control and LPS-treated wild type animals is indicated by ± (p < 0.05), significant difference between LPS-treated wild type and CypD knock-out animals is indicated by * (p < 0.05).

3.7. CypD knock-out mice do not exhibit prominent NF-κB activation after LPS treatment

We determined the phosphorylation level of the p65 subunit of NF-κB and inhibitory-κB (IκB). LPS caused a significant activation of NF-κB in wild type mice compared to CypD$^{-/-}$ animals (Figure 7A). Similarly, robust IκB phosphorylation was found in wild type animals after LPS treatment; however, CypD$^{-/-}$ mice showed decreased phosphorylation, which seems to confirm our data regarding NF-κB activation (Figure 7B).
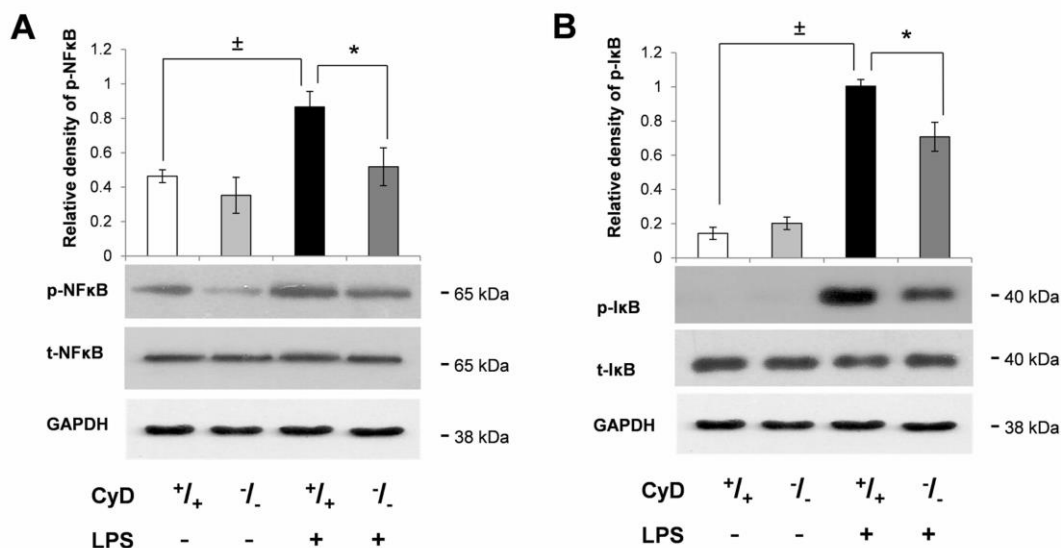
**Figure 7. CypD is required for LPS-induced NF-κB activation.** Phosphorylation of NF-κB (A) and IκB (B) in lung total homogenates was determined 24 h after LPS treatment by immunoblotting, utilizing phosphorylation specific primary antibodies. Total proteins (non-phosphorylated) and GAPDH were used as loading controls. A representative blot as well as a bar diagram of the quantified blots are presented. Bars represent mean ± SEM of pixel

329 densities, n = 4. Significant difference between control and LPS-treated wild type animals is
330 indicated by ± (p < 0.001), significant difference between LPS-treated wild type and CypD
331 knock-out animals is indicated by * (P < 0.05).

332

3.8. Marked differences between wild type and CypD knock-out animals regarding NF-κB-mediated gene expression

335 To gain further insight into the functional inhibition of NF-κB, we determined the gene
336 expression of NF-κB-regulated inflammatory mediators that are crucial in the
337 pathophysiology of LPS-induced ALI using qRT-PCR. Expression of CD14, CXCl2, IFNγ,
338 TNFα, IL-1 and inducible NO synthase (iNOS) was elevated in LPS-treated wild type
339 animals; this LPS-induced overexpression was strongly reduced in every case in the knock-
340 out mice. Our data show that NF-κB regulation in CypD$^{-/-}$ animals is not limited to the level
341 of phosphorylation of key signaling enzymes, but it affects the transcription of the related
342 genes as well (Figure 8).

343
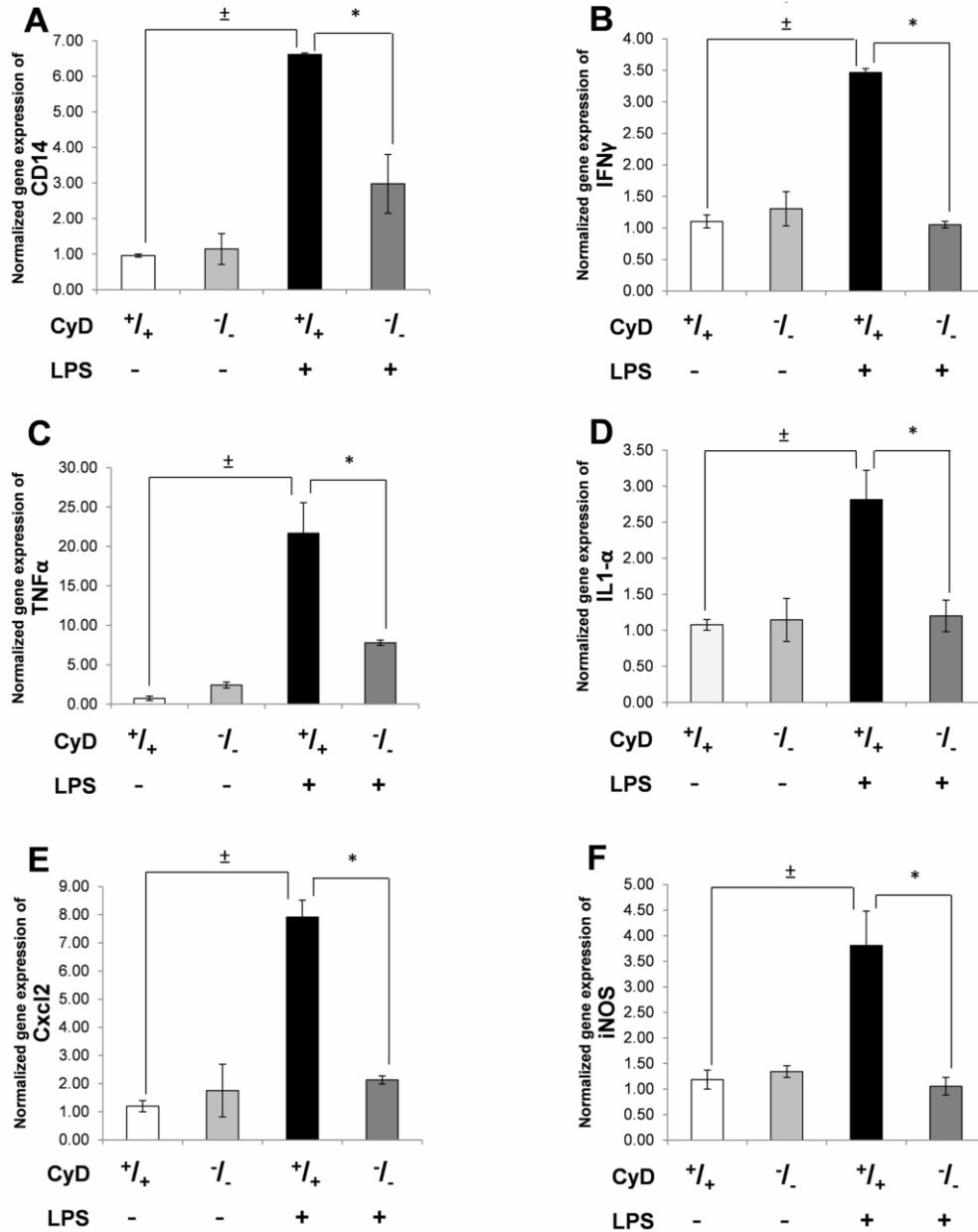
Figure 8. CypD regulates LPS-induced NF-κB-mediated gene expression. The expression
of NF-κB-mediated inflammatory genes, CD14 (A), IFN-γ (B), TNFα (C), IL-1α (D), Cxcl2
(E) and iNOS (F) was determined 24h after LPS treatment in lung tissue by RT-PCR. Actin
was used as a housekeeping gene to generate the ΔCt values. Data were normalized to ΔCt
values of untreated controls. Results are presented as mean ± SEM, n = 4. Significant
difference between control and LPS-treated wild type animals is indicated by ± ($p < 0.001$),
significant difference between LPS-treated wild type and CypD knock-out animals is
indicated by * ($P < 0.05$).

4. Discussion

20

354

In the present study, we demonstrated that a deficiency of CypD ameliorates pathological consequences of endotoxemia-induced ALI, both at the tissue and molecular levels, and massively reduces mortality rate. Cyclophilins are ubiquitous proteins differing in their subcellular localization and binding affinity to CsA. CsA inhibits calcineurin thereby suppresses MKP-1 expression resulting in increased MAPK activation [27]. Therefore, considering the importance of MAPKs in NF-κB activation, CsA is obviously unsuitable for studying the effect of mPT impairment on LPS-induced inflammatory response. To resolve this problem and to focus on the role of CypD and mPT on LPS-induced inflammation, we used a CypD$^{-/-}$ model.

LPS is known to cause excessive inflammatory response with oxidant-antioxidant imbalance in many organs, severely affecting the lungs. Lung epithelial cells and macrophages, as well as sequestered neutrophils produce excessive amounts of ROS, amplifying oxidant events. Mitochondrial ROS production-induced cellular damage has been implicated in the pathophysiology of LPS-induced inflammation and ALI [28] characterized by endothelial barrier dysfunction, interstitial edema and thickening, epithelial damage, and the accumulation of neutrophils. Our histological results showed the same characteristics in the lungs of LPS-challenged wild type mice, but animals lacking CypD showed only mild tissue injury. Histological scores supported these findings. The deleterious effect of ROS on endothelial and epithelial morphology and barrier function has been demonstrated at the subcellular fine structural level using electron microscopy; however, a definitive protective effect was found in CypD-deficient mice. Our results suggest that the loss of CypD greatly diminishes ROS and RNS production after LPS treatment with the consequent attenuation of microscopic and subcellular pathological changes and oxidative tissue damage in the lungs of mice.

ROS contribute to the inflammatory phenotype, with the increased production of proinflammatory cytokines in lung cells. Elevated concentrations of proinflammatory chemokines and cytokines, including IL-8, IL-1β, and TNFα, in the lungs are critical regulators of the outcome of ALI. Compared to wild type animals, in CypD-deficient mice, the level of TNFα and IL-1β produced by resident cells was decreased, indicating that the lack of CypD could severely interfere with cytokine generation, possibly due to reduced mitochondrial ROS production. This strong correlation between mitochondrial ROS and

proinflammatory cytokine production was also reported by Bulua and his coworkers, pointing to the fact that the blockade of mitochondrial ROS generation efficiently reduces inflammatory cytokine production after treatment in cells from patients with TNF receptor-associated periodic syndrome and from healthy individuals [29].

As a counterbalance, IL-10 is a key anti-inflammatory cytokine in the down-regulation of inflammatory response. One of its key functions is regulation of the pathogen-mediated activation of macrophages and dendritic cells, consequentially inhibiting the expression of chemokines, inflammatory enzymes, and potent proinflammatory cytokines. Elevated levels of IL-10 after LPS exposure did not differ in the two LPS-treated groups, indicating that the ameliorated inflammatory processes in CypD-deficient animals are not a consequence of anti-inflammatory mechanisms but of attenuated ROS production.

ROS are important chemical mediators that regulate signal transduction pathways, including members of the MAP kinases. In line with previous studies, [25, 26] we found the increased phosphorylation of MAPKs in the lungs after LPS treatment. Phosphorylation of redox-sensitive p38 and ERK was markedly decreased in CypD-deficient mice; however, JNK activation was unaltered in our experiments. Although ROS could activate all three MAPKs, this regulation is conducted by different upstream regulators independently of each other. It was previously reported that H_2O_2 stimulates JNK but not p38 and ERK via a pathway that is dependent on Src; however, the exact mechanisms for ROS-mediated p38 and ERK activation remain unknown [30]. Based on our results the depletion of CypD exerts its effect on ROS-induced MAPK activation in p38- and ERK-dependent and JNK-independent ways. Besides the regulation of upstream mediators of MAPKs, direct control mechanisms could act also through MKP-1 activity. MKP-1 is a central redox sensitive regulator of ERK and p38 during endotoxemia, ameliorating monocyte activation and consequential lung injury [31, 11]. Up-regulation of MKP-1 in CypD knock-out mice upon LPS exposure represents a strong protective pathway due to the attenuated activation of ERK and p38. Previous studies have shown that p38 is regulated by Akt as well, positively influencing NF-κB activation [32]. Indeed, the phosphorylation pattern of p38 followed that of Akt in our experiments. Since Akt could be activated by ROS [33] and IL-1β [32], a lack of CypD could down-regulate the Akt-p38-NF-κB pathway through these inflammatory mediators. In accordance with these findings, NF-κB and IκB phosphorylation increased dramatically after LPS treatment in the lungs of wild type but not CypD-deficient animals. Moreover, we proved the functional inhibition of NF-κB activity in the absence of CypD, analyzing NF-κB-related genes at the

mRNA and protein levels. In CypD-deficient mice, the expression of important participants of TLR4 signaling (CD14, iNOS) and mediators of ALI, like chemokines and cytokines (Cxcl2, IFNγ, TNFα, IL-1α), showed a significant decrease compared to wild type animals. Our gene expression data suggest that the downregulation of NF-κB and the related genes by the lack of CypD may be essential to prevent or treat inflammatory diseases.

In summary, we demonstrate that the loss of essential mPT modulatory protein CypD can intensely ameliorate endotoxemia-induced lung injury in mice through down-regulation of the NF-κB pathway, inflammatory mediators and reducing the production of ROS. Our data highlight a previously unknown regulatory function of mitochondria due to the mediation of mPT during inflammatory responses. This finding offers a valuable therapeutic target in conditions of acute inflammation including ALI.

Conflict of interest

The authors declare no conflict of interest.

Acknowledgements

References

1. Brigham KL, Meyrick B. (1986) Endotoxin and lung injury. Am Rev Respir Dis 133: 913-927.

2. Takeuchi O, Hoshino K, Kawai T, Sanjo H, Takada H, et al. (1999) Differential roles of TLR2 and TLR4 in recognition of gram-negative and gram-positive bacterial cell wall components. Immunity 11: 443-451.

3. Lu YC, Yeh WC, Ohashi PS. (2008) LPS/TLR4 signal transduction pathway. Cytokine 42: 145-151.

4. Togbe D, Schnyder-Candrian S, Schnyder B, Doz E, Noulin N, et al. (2007) Toll-like receptor and tumour necrosis factor dependent endotoxin-induced acute lung injury. Int J Exp Pathol 88: 387-391.

5. Blackwell TS, Holden EP, Blackwell TR, DeLarco JE, Christman JW. (1994) Cytokine-induced neutrophil chemoattractant mediates neutrophilic alveolitis in rats: association with nuclear factor kappa B activation. Am J Respir Cell Mol Biol 11: 464-472.

6. Blackwell TS, Christman JW. (1997) The role of nuclear factor-kappa B in cytokine gene regulation. Am J Respir Cell Mol Biol 17: 3-9.

7. Grommes J, Soehnlein O. (2011) Contribution of neutrophils to acute lung injury. Mol Med 17: 293-307.

8. Veres B, Gallyas F Jr., Varbiro G, Berente Z, Osz E, et al. (2003) Decrease of the inflammatory response and induction of the Akt/protein kinase B pathway by poly-(ADP-ribose) polymerase 1 inhibitor in endotoxin-induced septic shock. Biochem Pharmacol 65: 1373-82.

9. Veres B, Radnai B, Gallyas F Jr., Varbiro G, Berente Z, et al. (2004) Regulation of kinase cascades and transcription factors by a poly(ADP-ribose) polymerase-1 inhibitor, 4-hydroxyquinazoline, in lipopolysaccharide-induced inflammation in mice. J Pharmacol Exp Ther 310: 247-55.

10. Jakus PB, Kalman N, Antus C, Radnai B, Tucsek Z, et al. (2013) TRAF6 is functional in inhibition of TLR4-mediated NF-κB activation by resveratrol. J Nutr Biochem 24: 819-23.

11. Tucsek Z, Radnai B, Racz B, Debreceni B, Priber JK, et al. (2011) Suppressing LPS-induced early signal transduction in macrophages by a polyphenol degradation product: a critical role of MKP-1. J Leukoc Biol 89: 105-111.

12. Crompton M. (1999) The mitochondrial permeability transition pore and its role in cell death. Biochem J 341: 233-249.

13. Giorgio V, von Stockum S, Antoniel M, Fabbro A, Fogolari F, et al. (2013) Dimers of mitochondrial ATP synthase form the permeability transition pore. Proc Natl Acad Sci U S A 110: 5887-92.

14. Baines CP, Kaiser RA, Purcell NH, Blair NS, Osinska H, et al. (2005) Loss of cyclophilin D reveals a critical role for mitochondrial permeability transition in cell death. Nature 434: 658-662.

15. Basso E, Fante L, Fowlkes J, Petronilli V, Forte MA, et al. (2005) Properties of the permeability transition pore in mitochondria devoid of Cyclophilin D. J Biol Chem 280: 18558-18561.

16. Camara AK, Lesnefsky EJ, Stowe DF. (2010) Potential therapeutic benefits of strategies directed to mitochondria. Antioxid Redox Signal 13: 279-347.

17. Naoumov NV. (2014) Cyclophilin inhibition as potential therapy for liver diseases. J Hepatol 61: 1166-1174.

488   18. Nigro P, Pompilio G, Capogrossi MC. (2013) Cyclophilin A: a key player for human
489   disease. Cell Death Dis 4: e888.
490   19. Jeong K, Kim H, Kim K, Kim SJ, Hahn BS, et al. (2014) Cyclophilin B is involved in
491   p300-mediated degradation of CHOP in tumor cell adaptation to hypoxia. Cell Death
492   Differ 21: 438-50.
493   20. Fiedler B, Wollert KC. (2004) Interference of antihypertrophic molecules and signaling
494   pathways with the Ca^{2+}-calcineurin-NFAT cascade in cardiac myocytes. Cardiovasc
495   Res 63: 450-7.
496   21. Matute-Bello G, Downey G, Moore BB, Groshong SD, Matthay MA, et al. (2011) An
497   official American Thoracic Society workshop report: features and measurements of
498   experimental acute lung injury in animals. Am J Respir Cell Mol Biol 44: 725-738.
499   22. Meduri GU, Kohler G, Headley S, Tolley E, Stentz F, et al. (1995) Inflammatory
500   cytokines in the BAL of patients with ARDS. Persistent elevation over time predicts
501   poor outcome. Chest 108: 1303-1314.
502   23. Donnelly SC, Strieter RM, Reid PT, Kunkel SL, Burdick MD, et al. (1996) The
503   association between mortality rates and decreased concentrations of interleukin-10 and
504   interleukin-1 receptor antagonist in the lung fluids of patients with the adult
505   respiratory distress syndrome. Ann Intern Med 125: 191-196.
506   24. Wu CL, Lin LY, Yang JS, Chan MC, Hsueh CM. (2009) Attenuation of
507   lipopolysaccharide-induced acute lung injury by treatment with IL-10. Respirology
508   14: 511-521.
509   25. Bozinovski S, Jones JE, Vlahos R, Hamilton JA, Anderson GP. (2002)
510   Granulocyte/macrophage-colony-stimulating factor (GM-CSF) regulates lung innate
511   immunity to lipopolysaccharide through Akt/Erk activation of NFkappa B and AP-1 in
512   vivo. J Biol Chem 277: 42808-42814.
513   26. Kim HJ, Lee HS, Chong YH, Kang JL. (2006) p38 Mitogen-activated protein kinase up-
514   regulates LPS-induced NF-kappaB activation in the development of lung injury and
515   RAW 264.7 macrophages. Toxicology 225: 36-47.
516   27. Lim HW, New L, Han J, Molkentin JD. (2001) Calcineurin enhances MAPK phosphatase-
517   1 expression and p38 MAPK inactivation in cardiac myocytes. J Biol Chem 276:
518   15913-9.
519   28. Richter C, Gogvadze V, Laffranchi R, Schlapbach R, Schweizer M, et al. (1995) Oxidants
520   in mitochondria: from physiology to diseases. Biochim Biophys Acta 1271: 67-74.
521   29. Bulua AC, Simon A, Maddipati R, Pelletier M, Park H, et al. (2011) Mitochondrial
522   reactive oxygen species promote production of proinflammatory cytokines and are
523   elevated in TNFR1-associated periodic syndrome (TRAPS). J Exp Med 208: 519-533.
524   30. Yoshizumi M, Abe J, Haendeler J, Huang Q, Berk BC. (2000) Src and Cas mediate JNK
525   activation but not ERK1/2 and p38 kinases by reactive oxygen species. J Biol Chem
526   275: 11706-11712.
527   31. Kim HS, Ullevig SL, Zamora D, Lee CF, Asmis R. (2012) Redox regulation of MAPK
528   phosphatase 1 controls monocyte migration and macrophage recruitment. Proc Natl
529   Acad Sci U S A 109: E2803-2812.
530   32. Madrid LV, Mayo MW, Reuther JY, Baldwin AS Jr. (2001) Akt stimulates the
531   transactivation potential of the RelA/p65 Subunit of NF-kappa B through utilization of
532   the Ikappa B kinase and activation of the mitogen-activated protein kinase p38. J Biol
533   Chem 276: 18934-18940.
534   33. Lee SR, Yang KS, Kwon J, Lee C, Jeong W, et al. (2002) Reversible inactivation of the
535   tumor suppressor PTEN by H2O2. J Biol Chem 277: 20336-20342.
536